Odor Control Using Hollow Fiber Membrane Modules

Xiaoyao Tan and K. Li
Dept. of Chemical Engineering and Chemical Technology, Imperial College London, University of London, London SW7 2AZ, U.K.

W. K. Teo
Dept. of Chemical and Environmental Engineering, National University of Singapore, 10 Kent Ridge Road, Singapore-119260

DOI 10.1002/aic.10388
Published online March 10, 2005 in Wiley InterScience (www.interscience.wiley.com).

Odor control using hollow fiber membrane modules has been investigated both theoretically and experimentally. First, a mathematical model for the odor gas removal from gas streams in hollow fiber membrane modules was developed, with which the effects of the liquid flow rate and the reactant concentration in solution on the odor removal were studied. As a result, a criterion to determine the optimum liquid flow rate and reactant concentration required for the odor removal was established. Second, experimental studies on the odor removal, that is, H_2S removal from N_2 streams in PVDF hollow fiber membrane modules were carried out. The results indicate that H_2S with low concentrations can be removed from gas streams effectively and economically, and a very high removal rate could be expected. All the experimental data can be estimated satisfactorily with the presented mathematical model. Finally, application of the hollow fiber membrane module fitted in air conditioners for the indoor air purification was explored and a quick graphic method for designing the membrane module was presented. *AIChE J,* 51: 1367–1376, 2005
Keywords: odor control; hollow fiber membranes; indoor air purification

Introduction

Odor control is a very important environmental topic and is getting increasing concern in the worldwide. Odor emissions are often associated with waste products, either by industry or domestic household, such as treatment of municipal sewage. The gas compounds produced from domestic wastewater commonly include hydrogen sulfide (H_2S), ammonia (NH_3), aldehydes, and so on. There are generally three features of odorous gas streams: (1) the concentration of the odor compounds is very low; (2) the gas-stream volume is large, and (3) the gas stream pressure is low. In addition, natural gas, refinery gas or coal gas, commonly employed for industrial and domestic heating as well as for chemical processing contains hydrogen sulfide (H_2S) as one of their major impurities. Hydrogen sulfide is a highly toxic and corrosive gas and is one of the major sources for the environmental problem of acid rain. In order to control or to eliminate the odor emission from sewage treatment plant, and to utilize these fuel gases for chemical processing or energy generation, the concentration of these odors in gas streams must be reduced to a very low level: less than 0.0115 g/m^3 is required for some specific applications[1].

On the other hand, in tropical countries, such as Malaysia and Singapore, almost all the offices are in an air conditioned environment. It was reported that some people feel uncomfortable in staying in their office for long, mainly due to the indoor air pollutants, such as NH_3, carbon dioxide (CO_2), carbon monoxide (CO), formadehyde, and so on. Therefore, develop-

Correspondence concerning this article should be addressed to K. Li at Kang.Li@imperial.ac.uk.

ment of efficient odor removal and air cleaning technologies for the indoor air quality control is very important and also urgent.

Various conventional methods have been used to remove the odor compounds. The most common and economical process for purifying gas streams containing H_2S and other odor compounds are the gas absorption system (scrubbing). Absorption columns include packed or plate columns, spray chamber and jet scrubber. The packed tower currently is the most commonly used scrubbing equipment due to its low-pressure loss. The most common scrubbing medium is water with a chemical additive such as buffered potassium permanganate ($KMnO_4$), sodium hypocloride (NaOCl), caustic soda (NaOH), hydrogen peroxide (H_2O_2), chlorine (Cl_2), or ozone (O_3). In order to remove sufficiently the odor compounds, adequate contact time between the gas and scrubbing medium must be provided. In practice, packed tower has some limitations in separation efficiency and operation, and often suffers from flooding and loading at high or low gas/liquid flow rates.

Recent development in hollow fiber membrane modules provides an attractive alternative. The hollow fiber provides a barrier between gas and liquid. The gas components diffuse through membrane pores or membrane itself into the liquid phase. The microporous hollow fiber membranes employed for gas absorption or stripping provide several advantages compared to conventional absorption or stripping processes, such as bubble columns and packed beds. These include larger interfacial area per unit volume, independent control of gas and liquid flow rates without any flooding, loading, foaming, and so on, and known gas-liquid interfacial area. Recognition of these advantages is reflected by a number of investigations on the use of membrane modules for gas absorption and stripping reported in the literatures, by Zhang and Cussler [2,3], Yang and Cussler [4], Cooney and Jackson [5], Ahmed and Semmens [6], Kreulen et al.[7,8], Costello et al.[9] and Li et al.[10]. Moreover, due to the tangential nature of the flow in the membrane module, the gas absorption process does not require operation at a high-pressure drop. This contributes to lower capital cost and easier operation. Therefore, the hollow fiber membrane module is much beneficial in the treatment of gas streams containing low concentration of odor compounds and with a low stream pressure.

The objective of this work is to investigate the performances of hollow fiber membrane modules for odor removal under various operating conditions. Hydrophobic PVDF hollow fiber membranes with different morphological structures were prepared and characterized, and H_2S removal from N_2 gas streams was selected as an example for the odor control. The experimental data obtained were simulated with the mathematical model. Application of the hollow fiber membrane module, fitted in air conditioners for the indoor air quality control, was also explored, and a graphic method was outlined, which enables a quick estimate of the design parameters of such systems for the indoor air quality control.

Experimental

Preparation of PVDF hollow fiber membranes

Polyvinylidene fluoride (Kynar® grade 760, MW = 444,000) was used in pallet form and purchased from Elf Atochem (USA). Dimethylacetamide (DMAc) (Merck, 99+%) was used as the solvent. The additives used include LiCl and nonsolvent, such as water, ethanol, acetic acid and propionic acid. Water was used as both the internal and the external coagulants.

Different compositions of polymer dopes consisting of PVDF, DMAc, and additives were prepared. When using LiCl as an additive, the solid LiCl was first dissolved in DMAc according to the predetermined amount. The PVDF was then dissolved in DMAc and/or the mixture of DMAc/LiCl at about 333 K. After the PVDF was completely dissolved, the nonsolvent was added at the room-temperature (298 ± 1 K) under agitation and was further mixed for at least 1 day. The polymer dopes prepared are clear and homogeneous at room temperature.

The hollow fiber spinning apparatus and detail spinning procedures have been described elsewhere[11]. The fibers were spun by a dry/wet or wet spinning process at the room-temperature (298±1 K). The take-up velocity is 4-5 m/min. The solution extrusion rate is in the range of 1.2 to 1.5 cm^3/min, and the internal coagulant flow rate is in the range of 1.5 to 2 cm^3/min. The prepared hollow fibers were immersed in fresh water for at least 2 days and then examined for their properties.

Characterization of the membranes

The mean pore radius, r_m standard deviation σ and the effective surface porosity, ε/L_p (defined as ratio of the surface porosity to the effective pore length) are the very important parameters in determining an asymmetric membrane resistance. These parameters were determined from the dried membranes using an improved gas permeation method developed by Kong and Li [12]. The wet hollow fibers were dried at the ambient condition (298 ± 1 K and RH = 60 – 65%). Large shrinkage was observed when the membranes were dried. In order to reduce the membrane shrinkage, some water-wet membranes were treated by an organic nonsolvent exchange method before air-drying. A test module with the length of about 6 cm and containing 2–10 fibers was made. The test apparatus used was based on the volume displacement method. The upstream pressure was in the range from 34.3 kPa to 206.1 kPa, which was measured by the pressure transducer (Basingstoke, England). Nitrogen gas was used as a standard gas and the permeation flux was measured at 298 ±1 K and atmosphere using a soap-bubble flow meter. The gas permeation data obtained at different operating pressures were analyzed using the technique developed [12]. The results of r_m, σ and ε/L_p were then obtained and were given in Table 1.

Experimental apparatus and procedures for the odor removal

The experimental setup for the removal of odor gases, such as H_2S is shown in Figure 1, where the hollow fiber module was made up of 9 PVDF hollow fibers using the membrane 8 in Table 1, with an effective length of 27.25 cm. A feed gas mixture containing the odor gas (H_2S) in balance with N_2 was introduced into the fiber lumen at a desired flow rate. The inlet gas flow rate was monitored by a mass flow sensor (5860E series, Brooks), while the outlet gas flow rate was controlled using a mass flow controller (5850E series, Brooks®). An aqueous Na_2CO_3 solution used as the absorbing liquid was introduced into the shell side of the hollow fiber module, and

Table 1. Properties of the Spinning Solution and the Resulting Hollow Fiber Membranes: Effects of LiCl and Nonsolvent Additives

Membrane	1	2	3	4	5	6	7	8	9
Composition of spinning solution (wt%)									
PVDF (Kynar® K760)	14.1	13.8	13.4	12.9	13.9	13.6	13.4	15	15
DMAc	80.2	78.0	75.9	73.3	78.7	77.3	75.9	77.8	72.6
Lithium chloride (LiCl)	5.7	5.5	5.4	5.2	5.6	5.5	5.4	5.2	5.2
Acetic acid (Hac)	—	2.8	5.4	8.6	—	—	—	—	—
Propionic acid (PAc)	—	—	—	—	1.9	3.6	5.4	—	—
Water	—	—	—	—	—	—	—	2.0	—
Ethanol	—	—	—	—	—	—	—	—	7.2
Membrane's properties									
Outer diameter $\times 10^3$, m	0.80	0.78	0.71	0.65	0.76	0.76	0.73	0.91	0.7
Inner diameter $\times 10^3$, m	0.52	0.48	0.43	0.40	0.44	0.44	0.43	0.61	0.42
Mean pore radius $\times 10^6$, m	0.061	0.081	0.052	0.094	0.057	0.073	0.065	0.044	0.043
Effective surface porosity, ε/L_p, m^{-1}	840	1020	1510	1080	690	750	920	3700	3830
Standard deviation, σ	0.578	0.423	0.630	0.386	0.647	0.456	0.529	0.190	0.68

was in countercurrent contact with the feed gas. The flow rate of the liquid absorbent was controlled by a rotameter (Tokyo Keiso). Pressures at both the gas and liquid sides were maintained equally and no bubbles were observed in the liquid side.

The outlet concentration of the odor gas (H_2S) was measured using the Continuous Toxic Gas Monitor (Model 7100 from Zellweger Analytics) at an interval of 6 min. All data were obtained at steady state after sufficient operating time was allowed for system stabilization. Three samples were taken under the same operating conditions and the average value was calculated. The deviation between the sample values and the average value is less than 5%.

Theory

The mathematical model developed in the following is based on the actual operating mode: gas stream containing odor gas is fed into the fiber lumen while the aqueous absorbing solution to the shell side of the module countercurrently, as shown in Figure 2. For simplification, subscripts A and B are used to represent the odor gas and the reactant in the aqueous solution, respectively.

Model equations

For the lumen feed and countercurrent operation mode, the concentration profile of the odor gas in the hollow fiber lumen can be written as

$$u\frac{\partial C_{Ag}}{\partial z} = D_{Ag}\left(\frac{1}{r}\frac{\partial C_{Ag}}{\partial r} + \frac{\partial^2 C_{Ag}}{\partial r^2}\right)$$

or

$$2u_m\left[1 - \left(\frac{r}{R_i}\right)^2\right]\frac{\partial C_{Ag}}{\partial z} = D_{Ag}\left(\frac{1}{r}\frac{\partial C_{Ag}}{\partial r} + \frac{\partial^2 C_{Ag}}{\partial r^2}\right) \quad (1)$$

with the boundary conditions

$$r = 0, \quad \frac{\partial C_{Ag}}{\partial r} = 0, \quad r = R_i, \quad D_{Ag}\frac{\partial C_{Ag}}{\partial r} = -\frac{dN_A}{2\pi R_i dz} \quad (1a)$$

$$z = 0, \quad C_{Ag} = C_{Af} \quad (1b)$$

where u_m is the average gas velocity, m/s, $u_m = (V_G/n\pi R_i^2)$; V_G is the volumetric flow rate of gas mixture, m^3/s; n is the number of hollow fibers in the module; R_i is the inner radius of the hollow fiber, m; N_A is the molar flow rate of odor gas permeating through the membrane, mol/s; D_{Ag} is the bulk diffusivity of odor gas in the gas phase, m^2/s; C_{Ag} and C_{Af} are the local concentration of odor gas in the fiber lumen and the feed concentration, respectively, mol/m^3.

It should be noted that the above equation was written with the assumptions of: (1) fully developed laminar flow in the tube (lumen) side, (2) negligible axial diffusion in the tube side, (3)

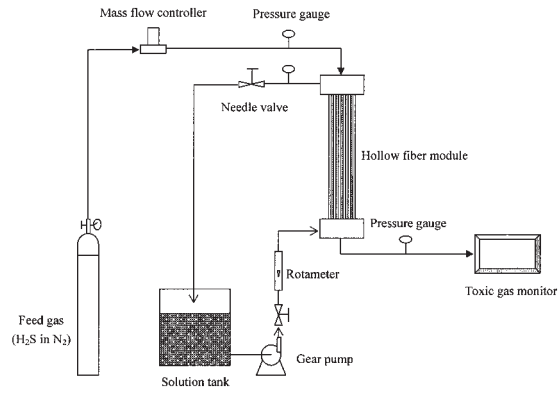

Figure 1. Set-up for the removal of odor gas.

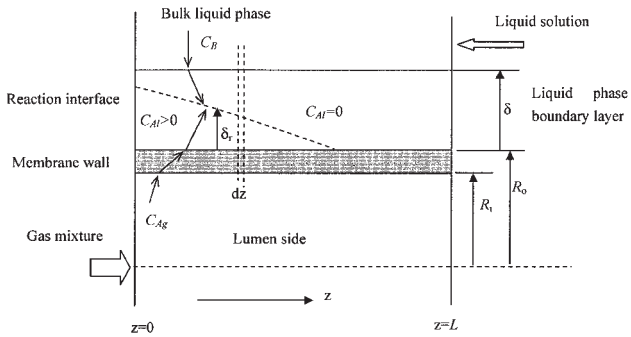

Figure 2. Mass transfer diagram for odor removal in one hollow fiber membrane.

constant tube- and shell- side pressures, and (4) the steady state and isothermal operating system. Assumption (1) is valid for Reynolds number not exceeding 2100, which is true for the small diameter of the fibers used. Assumption (2) is admissible since the flow velocity in the tube side can be generally expected to be greater than axial diffusion.

In the shell side, the liquid flow rate almost remains constant because the concentration of odor gas is very low. Therefore, the conservation equation for the reactant in the absorbing liquid may be given by

$$\frac{V_L dC_B}{b} = n \cdot dN_A \tag{2}$$

with the boundary condition

$$z = L, \quad C_B = C_{Bf} \tag{2a}$$

where V_L is the volumetric flow rate of aqueous absorbing solution, m^3/s; L is the length of the fiber, m; b is the stoichiometric coefficient; C_B and C_{Bf} are the concentrations of absorbing reactant in the solution and in the liquid feed, respectively, mol/m^3.

In the case of purely physical absorption, Eq. 2 can then be replaced with the conservation equation of odor gas in the solution as

$$V_L dC_A = -n \cdot dN_A \tag{3}$$

with the boundary condition

$$z = L, \quad C_A = 0 \tag{3a}$$

The bulk average or "mixing cup" values of gas concentration is:

$$\bar{C}_{Ag} = \frac{\int_0^{R_i} C_{Ag} u \cdot 2\pi r dr}{\int_0^{R_i} u \cdot 2\pi r dr} = \frac{4}{R_i^2} \int_0^{R_i} C_{Ag}[1 - (r/R_i)^2] r dr \tag{4}$$

The extent of the odor gas removal is generally defined as

$$\sigma_t = 1 - \frac{\bar{C}_{Ag}|_{z=L}}{C_{Af}} \tag{5}$$

Permeation rate of the odor gas through the membrane

For the hydrophobic membranes such as PVDF, the gas mixture is filled within the membrane pores. The permeation rate of an odor gas through a membrane in a differential hollow fiber length is given by

$$dN_A = \frac{2\pi k_{Am}(R_o - R_i)}{\ln(R_o/R_i)} \cdot (C_{Ag}|_{r=R_i} - C_{Ag}|_{r=Ro}) dz \tag{6}$$

where R_o is the outer radius of the hollow fiber, m; $C_{Ag}|_{r=R_i}$ and $C_{Ag}|_{r=R_o}$ C are the concentrations of the odor gas at the inner and outer surfaces of the fiber membrane, respectively, mol/m^3 and k_{Am} is the membrane's mass-transfer coefficient, m/s.

Since gas mass transfer through porous asymmetric hollow fiber membranes with an integral skinned layer are mainly governed by the morphology of the skin layer and the porous substrates have less resistance, for non-wetted microporous membranes, that is, gas-filled pores, the membrane's mass-transfer coefficient can be evaluated independently using the pore structure properties of the membrane [12]

$$k_{Am} = D_{Am} \cdot \frac{\varepsilon_p}{L_p} \tag{7}$$

in which D_{Am} is the diffusivity of the odor gas in the membrane m^2/s, which is governed by both bulk diffusion and Knudsen diffusion. Considering that the real pore-size distribution of porous membranes may be represented by the log-normal distribution [13,14], the effective diffusivity of odor gas in the membrane can be expressed by [15]

$$D_{Am} = D_{Ag} \times \frac{\int_0^{\infty} r^2/(\alpha + r)\exp[-(\ln(r/r_m)(1 + \sigma^2)^{0.5})^2/(2\ln(1 + \sigma^2))]dr}{\int_0^{\infty} r \exp[-(\ln(r/r_m)(1 + \sigma^2)^{0.5})^2/(2\ln(1 + \sigma^2))]dr} \tag{8}$$

where r_m (m) and σ are the mean pore radius and standard deviation of the membrane, respectively. α (cm) is defined as[15]

$$\alpha = \frac{1.5 \times 10^{-4} D_{Ag}}{\sqrt{8\Re T/\pi M_A}} \tag{8a}$$

in which is $\Re$ gas constant, 8.314 J/mol K; M_A is the molecular weight of odor gas Kg/mol.

Absorption rate of odor gas with chemical reaction

In general, the reaction between odor gas and the reactant in the absorbing solution can be written as

$$\mathrm{A} + \mathrm{bB} \Rightarrow \mathrm{C} \tag{i}$$

For odor gases, such as H_2S and NH_3, the reaction can be considered to be instantaneous[16]. Therefore, the location of the reaction plane (that is, a distance, δ_r away from the membrane's outer surface) is dependent on both the odor (A), and the absorbing reactant (B) concentrations in the liquid phase, and is illustrated as the dashed line in Figure 2. Since the concentrations of A and B are both equal to zero on the reaction plane, the absorption rate of odor gas can be written as

$$dN_A = 2\pi r dz \cdot \left(-D_{Al} \frac{\partial C_A}{\partial r} \right) \tag{9}$$

with the boundary condition

$$r = R_o, \quad C_A = C_{Ag}|_{r=R_o}/H_A; \quad r = R_o + \delta_r, \quad C_A = 0 \tag{9a}$$

Integrating Eq. 9 gives

$$dN_A = 2\pi D_{Al} \cdot \frac{C_{Ag}|_{r=R_o}/H_A}{\ln(1 + \delta_r/R_o)} dz \tag{10}$$

where D_{Al} is the diffusivity of the odor gas in liquid phase, m^2/s; H_A is the Henry's constant of the odor gas in water, and δ_r is the distance of the reaction plane (away from the membrane's outer surface, m).

Combining Eq. 10 with Eq. 6 yields the local disappearance rate of the odor gas as

$$dN_A = 2\pi \cdot \frac{C_{Ag}|_{r=R_i}}{\dfrac{\ln(R_o/R_i)}{k_{Am}(R_o - R_i)} + \dfrac{H_A}{D_{Al}} \ln(1 + \delta_r/R_o)} dz \tag{11A}$$

In the two special cases, the purely physical absorption and the surface reaction absorption processes, the local disappearance rate of odor gas may be then easily given, respectively, by

$$dN_A = 2\pi \cdot \frac{C_{Ag}|_{r=R_i} - H_A C_A}{\dfrac{\ln(R_o/R_i)}{k_{Am}(R_o - R_i)} + \dfrac{H_A}{D_{Al}} \ln(1 + \delta/R_o)} dz$$

(for purely physical absorption) (11B)

and

$$dN_A = 2\pi \cdot \frac{C_{Ag}|_{r=R_i}}{\dfrac{\ln(R_o/R_i)}{k_{Am}(R_o - R_i)}} dz$$

(for surface reaction absorption) (11C)

The diffusion rate of the adsorbing reactant from bulk liquid phase to the reaction plane may be written as

$$dN_B = 2\pi r dz \cdot \left(-D_{Bl} \frac{\partial C_B}{\partial r} \right) \tag{12}$$

with the following boundary condition

$$r = R_o + \delta_r, \quad C_B = 0; \quad r = R_o + \delta, \quad C_B = C_B \tag{12a}$$

Integrating the earlier equation yields

$$dN_B = -2\pi D_{Bl} \cdot \frac{C_B}{\ln \dfrac{R_o + \delta}{R_o + \delta_r}} dz \tag{13}$$

where D_{Bl} is the diffusivity of the reactant in the absorbing solution, m^2/s.

On the basis of the stoichiometric equation (Eq. i), $dN_A = -dN_B/b$, namely

$$\frac{bC_{Ag}|_{r=R_i}}{\dfrac{1}{k_{Am}(R_o - R_i)} \ln \dfrac{R_o}{R_i} + \dfrac{H_A}{D_{Al}} \ln \dfrac{R_o + \delta_r}{R_o}} = \frac{C_B}{\dfrac{1}{D_{Bl}} \ln \dfrac{R_o + \delta}{R_o + \delta_r}} \tag{14}$$

Therefore, the distance of the reaction plane, δ_r is dependent on the local concentrations of the reactants and the boundary layer thickness as well, and may be determined by

$$\frac{\delta_r}{R_o} = \begin{cases} \exp\left[\dfrac{\ln(1 + \delta/R_o) - \dfrac{D_{Bl} C_B \ln(R_o/R_i)}{k_{Am} b C_{Ag}|_{r=R_i}(R_o - R_i)}}{1 + \dfrac{D_{Bl} H_A}{D_{Al}} \cdot \dfrac{C_B}{bC_{Ag}|_{r=R_i}}} \right] - 1 & \text{for } \dfrac{D_{Bl} C_B}{\ln(1 + \delta/R_o)} < \dfrac{k_{Am} b C_{Ag}|_{r=R_i}(R_o - R_i)}{\ln(R_o/R_i)} \\ 0 & \text{for } \dfrac{D_{Bl} C_B}{\ln(1 + \delta/R_o)} \geq \dfrac{k_{Am} b C_{Ag}|_{r=R_i}(R_o - R_i)}{\ln(R_o/R_i)} \end{cases} \tag{15}$$

where δ is the boundary layer thickness, which is dependent on the hydrodynamics of the membrane system and may be estimated from the following correlation[9]

$$Sh = \frac{k_{Bl} d_e}{D_{Bl}} = \frac{d_e}{\delta} = (0.53 - 0.58\phi)\mathrm{Re}^{0.53} Sc^{0.33} \tag{16}$$

where ϕ is the packing fraction of hollow fibers in the module; *Re* and *Sc* are the Reynolds number and Schmidt number, respectively, and d_e is the characteristic dimension of the module m, which is defined as

$$d_e = \frac{4 \times \text{flow area}}{\text{total fiber circumference}} = \frac{D_s^2 - 4nR_o^2}{2nR_o} \tag{17}$$

where D_s is inner diameter of the module shell, m.

By performing the following dimensionless transforms

$$\eta = \frac{r}{R_i}, \quad \xi = \frac{z}{L}, \quad X_A = \frac{C_{Ag}}{C_{Af}}, \quad X_B = \frac{C_B}{C_{Bf}} \tag{18}$$

The governing Eqs. 1 and 2 then become

$$\frac{Gz}{2}(1-\eta^2)\frac{\partial X_A}{\partial \xi} = \frac{1}{\eta}\frac{\partial X_A}{\partial \eta} + \frac{\partial^2 X_A}{\partial \eta^2} \tag{19A}$$

$$Gz\frac{dX_B}{d\xi} = \frac{8Sh}{\beta_1\beta_2}\cdot X_A\big|_{\eta=1} \quad \text{(for chemical absorption)} \tag{19B}$$

The boundary conditions are rewritten in dimensionless form as

$$\eta = 0, \quad \frac{\partial X_A}{\partial \eta} = 0; \quad \eta = 1, \quad \frac{\partial X_A}{\partial \eta} = -Sh\cdot X_A \tag{20a}$$

$$\xi = 0, \quad X_A = 1; \quad \xi = 1, \quad X_B = 1 \tag{20b}$$

The depth of reaction plane is determined by

$$\frac{\delta_r}{R_o} = \begin{cases} \exp\left[\dfrac{X_A|_{\eta=1}\ln(1+\delta/R_o) - \gamma_1\gamma_2\beta_2 X_B}{X_A|_{\eta=1} + \gamma_1\beta_2 X_B}\right] - 1 & \text{for } X_A|_{\eta=1}\ln(1+\delta/R_o) \geq \gamma_1\gamma_2\beta_2 X_B \\ 0 & \text{for } X_A|_{\eta=1}\ln(1+\delta/R_o) < \gamma_1\gamma_2\beta_2 X_B \end{cases} \tag{21}$$

The dimensionless parameters defined in the above equations are listed in Table 2.

The extent of the odor gas removal in dimensionless form may be rewritten as

$$\sigma_t = 1 - 4\int_0^1 X_A|_{\xi=1}(1-\eta^2)\eta d\eta \tag{22}$$

The governing Eq. 19 can be transformed into a group of ordinary differential equations with two boundary values and can be integrated by the conventional numerical techniques, such as Runge-Kutta method [17]. A trial-calibration technique was used, and software of MATLAB was employed in this work.

Results and Discussion

In the following, the effects of liquid flow rate and reactant concentration in the absorbing solution on the odor removal were first studied with the mathematical model so as to optimize the operating conditions under which the maximum odor removal may be obtained. Following the theoretical studies, the experimental data for H_2S removal using PVDF hollow fiber membrane modules were computed and compared with the simulation results. Finally, the application of hollow fiber membrane modules to the indoor air purification was also presented and discussed. In order to obtain logical results, all the values of parameters used for the theoretical analysis were selected based on the experimental odor removal system, which are summarized in Table 3.

Table 2. Defined Dimensionless Parameters

Parameter	Expression
Graetz number, Gz	$\dfrac{u_m d_i^2}{D_{Ag}L}$
Feed modulus, β_1	$\dfrac{V_L}{V_G}$
Concentration modulus, β_2	$\dfrac{C_{Bf}}{bC_{Af}}$
Sherwood number, Sh	$\dfrac{1/D_{Ag}}{\dfrac{\ln(R_o/R_i)}{k_{Am}(R_o-R_i)} + \dfrac{\ln(1+\delta_r/R_o)}{D_{Al}/H_A}}$
γ_1	$\dfrac{D_{Bl}}{D_{Al}/H_A}$
γ_2	$\dfrac{D_{Al}/H_A}{k_{Am}(R_o-R_i)/\ln(R_o/R_i)}$

Theoretical analysis

As illustrated in Table 2, feed modulus β_1 is defined as the ratio of liquid flow rate to that of the gas stream, that is, $\beta_1 = V_L/V_G$. Meanwhile, the concentration modulus, β_2 is referred as the ratio of the reactant concentration in solution to the odor concentration in the gas feedstream, that is, $\beta_2 = C_{Bf}/bC_{Af}$. Note that the amount of the reactant fed in liquid solution must be more than the stoichiometric amount required for the complete removal of odor gas in the chemical stripping process, that is, $\beta_1\beta_2 \geq 1$, otherwise pure physical absorption occurs somewhere within the membrane module.

The odor removal at different feed and concentration moduli is shown in Figure 3 for three different Gz numbers (feed gas flow rate). In this figure, the dash-dotted, the dashed, the solid

Table 3. Characteristic Parameters of the Membrane Module for H_2S Removal

Number of fibers	$n = 9$
Length of the hollow fibers, m	$L = 27.25 \times 10^{-2}$
Module ID, m	$R_s = 0.435 \times 10^{-2}$
Fiber OD, m	$d_o = 9.07 \times 10^{-4}$
Fiber ID, m	$d_i = 6.07 \times 10^{-4}$
Average pore radius of the membrane, m	$r_m = 4.41 \times 10^{-8}$
Standard deviation of membrane pores	$\sigma = 0.19$
Effective porosity of the membrane, m^{-1}	$\varepsilon/L_p = 3700$
Operating temperature, K	$T = 298$
Henry's constant of H_2S in liquid	$H_A = 3.703 \times 10^{-3}$
Diffusivity of Na_2CO_3 in liquid, m^2/s	$D_{Bl} = 2.8 \times 10^{-9}$
Diffusivity of H_2S in liquid, m^2/s	$D_{Al} = 1.73 \times 10^{-9}$
Diffusivity of H_2S in nitrogen, m^2/s	$D_{Ag} = 1.677/P$ (Pa)

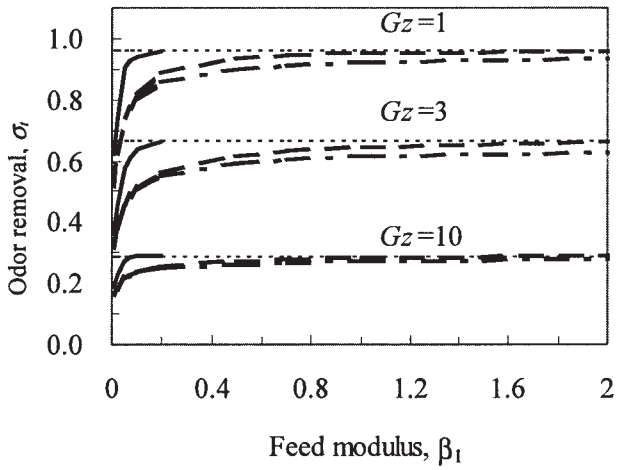

Figure 3. Effect of feed flow rate and reactant concentration on the odor gas removal (- -, purely physical absorption, $\beta_2 = 0$; - -:$\beta_2 = 10$; —: $\beta_2 = 50$; ·····: surface reaction process, $\beta_2 = \infty$).

and dotted lines represent the pure physical absorption ($\beta_2 = 0$), the chemical stripping process with $\beta_2 = 10$, the chemical stripping process with $\beta_2 = 50$, and the surface reaction process ($\beta_2 = \infty$), respectively. As is expected, the removal of odor gas increases as the feed modulus (liquid flow rate) or the concentration modulus (reactant concentration in solution) is increased. Obviously, the dotted line (namely the surface reaction process) represents the maximum odor removal for a given value of gas feed flow rate (Gz number). For the pure physical absorption process, the odor removal cannot reach the maximum value unless the liquid flow rate becomes infinite. However, this maximum odor removal can be achieved when the concentration modulus is increased to $\beta_2 = 10$, and the feed modulus approaches to $\beta_1 = 2$. However, if the liquid-flow rate is very low (that is, the feed modulus is less than 0.2), the enhancement of reaction on the odor removal is not obvious. Nevertheless, once the concentration modulus is increased to $\beta_2 = 50$, the maximum odor removal can be achieved at the feed modulus as low as 0.2. Therefore, it follows that the addition of reactant into the absorbing solution is capable of promoting the removal of odor gas and the amount of stripping solution can be drastically decreased.

The liquid feed flow rate (feed modulus) affects the removal of odor gas from two aspects. The first is that the thickness of fluid boundary layer adjacent to the membrane surface is decreased as the liquid flow rate increases. As a result, the resistance to the diffusion of both odor gas and reactant in solution decreases. Second, the large liquid flow rate implies that the local reactant concentration in solution would not decrease considerably along the module length and, thus, maintains a high overall driving force. Figure 4 shows the reaction plane profiles for different feed and concentration moduli. It can be seen that the reaction takes place in the liquid film when β_1 equals to 0.01, but on the membrane surface after z/L exceeds 0.88 for $\beta_1 = 0.02$, and 0.20 for $\beta_1 = 0.05$, respectively. Figure 4b shows the reaction plane profiles for the different concentration moduli. As would be expected, the increase of reactant concentration in solution promotes the driving force for its transport from the bulk liquid phase to the reaction plane, resulting in the closer reaction plane to the membrane surface and the faster absorption rate of odor gas.

For the countercurrent-operating mode, the reaction plane at the gas inlet of the module is away from the outer membrane surface at the farthest, because the odor concentration in the gas stream is highest, while the reactant concentration in the bulk liquid phase is lowest. Therefore, if the depth of reaction plane at the gas inlet of the module were zero, the reaction would take place on the outer membrane surface throughout the entire module. In another word, the liquid flow rate and the reactant concentration in solution must be carefully selected to satisfy the following expression so as to obtain the largest driving force for odor gas removal

$$\gamma_1\gamma_2\beta_2 X_B|_{\xi=0} \geq \ln(1 + \delta/R_o)$$

or

$$1 - \frac{\sigma_t}{\beta_1} \geq \frac{\ln(1 + \delta/R_o)}{\gamma_1\gamma_2} \tag{23}$$

in which the symbols are referred in the notation section.

The effect of gas velocity (Graetz number, $Gz = u_m d_i^2/D_{Ag}L$), liquid feed flow rate (feed modulus, β_1) and reactant concentration in the absorbing solution (concentration modulus, β_2) on the overall mass-transfer coefficient of the membrane module, in terms of overall Sherwood number, Sh_t =

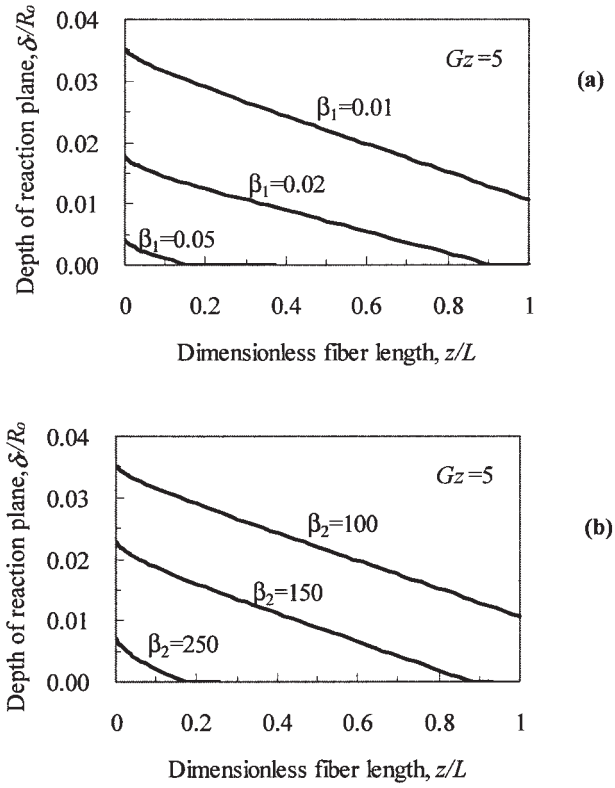

Figure 4. Reaction plane profiles: (a) for different feed moduli; and (b) for different concentration moduli.

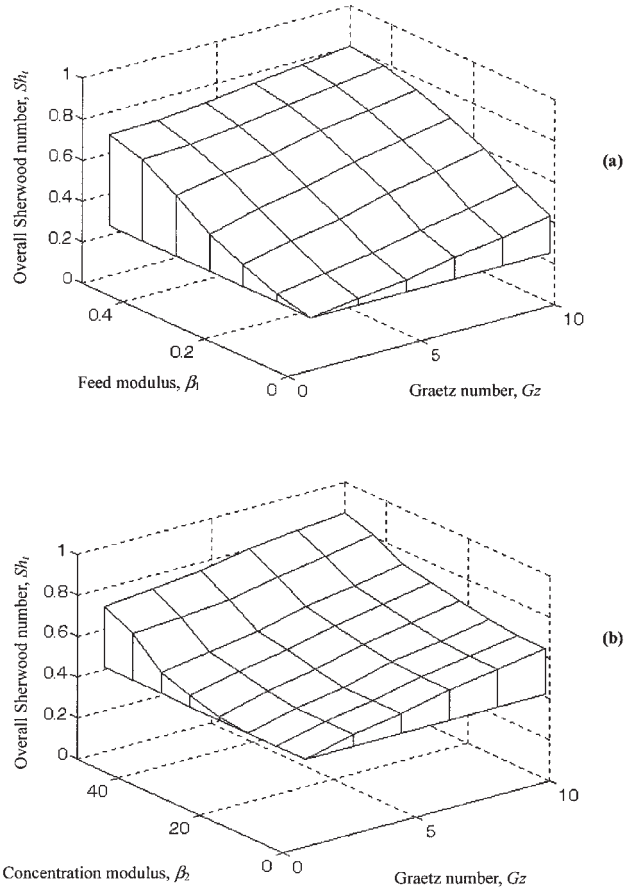

Figure 5. Overall Sherwood number against the feed and concentration modulus: (a) $\beta_2 = 10$; and (b) $\beta_1 = 0.1$.

$K_t d_m / D_{Ag}$, were also studied theoretically. Figure 5 shows the results. The concentration modulus was kept constant at $\beta_2 = 10$ in Figure 5a, while the feed modulus was kept constant at $\beta_1 = 0.1$ in Figure 5b. As can be seen, at the given operating conditions, the overall mass-transfer coefficient increases as the Graetz number (gas flow), the feed modulus (liquid flow) or the concentration modulus (reactant concentration) is increased. This result suggests that, at low gas and liquid flow velocities, as well as the low reactant concentration, the individual mass-transfer resistances in gas, liquid and membrane are not separated in wide magnitude, and all of them provide noticeable resistances to the mass transfer. As the Graetz number (gas flow), the feed modulus (liquid flow) and concentration modulus (reactant concentration) are increased, both the resistances in gas and liquid become negligible and membrane resistance controls the overall mass transfer as shown in Figure 5.

Experimental results

Figures 6 – 8 have shown the experimental results for the removal of H_2S from N_2 stream using the PVDF hollow fiber membrane modules at room temperature, in which the simulated results have also been presented. The values of parameters used for the theoretical calculation are listed in Table 3. Figure 6 shows the comparison of simulation results with the

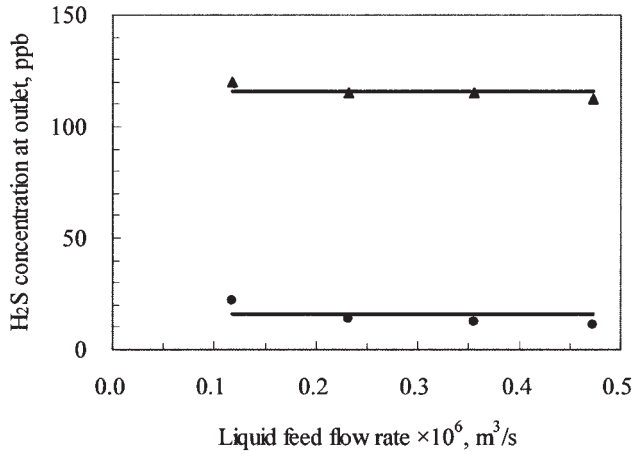

Figure 6. Effect of liquid feed flow rate on the residual concentration of H_2S (Experimental conditions: $P = 1.62 \times 10^5$ Pa, $C_{Bf} = 1.04 \times 10^3$ mol/m^3, ●- $V_G = 1.856 \times 10^{-5}$ m^3/s, $C_{Af} = 17.9$ ppm; ▲- $V_G = 1.484 \times 10^{-5}$ m^3/s, $C_{Af} = 1{,}000$ ppm).

experimental data for various liquid feed flow rates, while other operating conditions were kept constant. It can be seen from both theoretical and experimental results that H_2S concentration in the outlet stream remains unchanged as the liquid feed flow rate is increased. This indicates that the reaction takes place on the membrane surface throughout the module. Such a case can also be easily predicted using Eq. 23.

The effect of gas feed flow rate on the residual concentration of H_2S at different gas feed concentrations is shown in Figure 7. It shows that the residual concentration of H_2S is remarkably increased as the gas stream flow rate increases. This suggests that retention time of H_2S in the membrane module plays the key role in the absorbing process. Obviously, considering the system error, all the experimental data at various H_2S feed concentrations are in good agreement with the theoretical results.

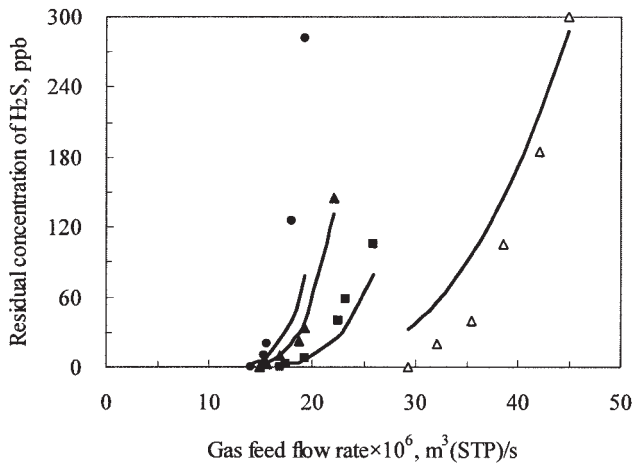

Figure 7. Effects of gas feed velocity on the H_2S removal (experimental conditions: $V_L = 7.5 \times 10^{-8}$ m^3/s, $P = 1.92 \times 10^5$ Pa, $C_{Bf} = 1.04 \times 10^3$ mol/m^3; Gas feed concentration: Δ-17.9 ppm; ■-100 ppm; ▲-580 ppm; ●-1159 ppm)).

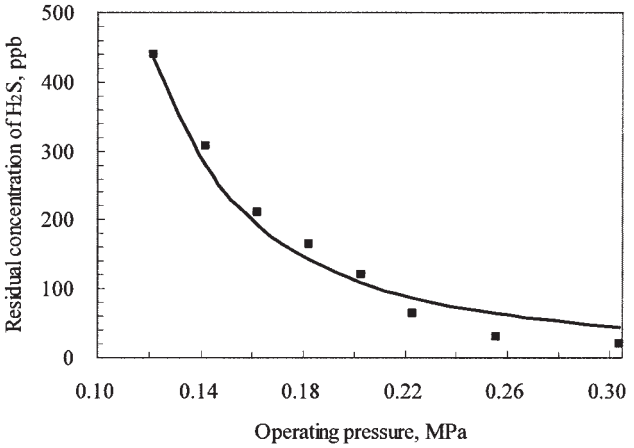

Figure 8. Effect of operating pressure on the H_2S depletion concentration (Experimental conditions: $V_G = 1.67 \times 10^{-5}$ m^3/s, C_{Af} = 1,000 ppm, $V_L = 2.53 \times 10^{-8}$ m^3/s, $C_{Bf} = 2 \times 10^3$ mol/m^3).

Figure 8 shows the effect of operating pressure on the residual concentration of H_2S. As can be seen, the H_2S concentration decreases as the operating pressure is increased. This is because that the velocity of gas stream within the modules decreases as the operating pressure is increased. Thus, the retention time of H_2S in the membrane module is increased. Although the diffusivity of H_2S in gas phase also decreases as the operating pressure is increased, resulting in lowering the mass-transfer coefficient, this effect is offset by the increase of retention time of H_2S in the membrane module. Such an effect has also been predicted exactly with this model, as shown in Figure 8. Therefore, in order to ameliorate the removal of odor gas, a slightly elevated operating pressure would be beneficial.

Application in the indoor air purification

A potential application of the hollow fiber membrane modules prepared is in the purification of indoor air. The hollow fiber membrane module can be installed within an air conditioner and the condensed water formed during the refrigeration may be used as the stripping solution. Since no reactant is present in the stripping solution, the pure physical stripping process takes place. Figure 9 illustrates the odor gas removal as a function of the operating number defined as $\beta = V_L / H_A V_G$ and the configuration number of the membrane module defined as $\gamma = K_t A_m / V_G$. It indicates that the odor gas removal is determined by both the gas and liquid flow rates, which are combined into operating number β, and also by the overall mass-transfer coefficient and membrane area, which are combined into configuration number, γ but independent of odor concentration in the gas stream. Furthermore, the maximum removal of odor gas is equal to the value of operating number at which the corresponding configuration number or the membrane area approaches to infinite. Obviously, in order to keep the room clean of odor gases, the removal rate of odor gas must be higher than the odor formation rate from office furniture such as photo copiers and printers or human bodies in the room, that is

$$V_G C_{Ag} \sigma_t > \upsilon_f \qquad (24)$$

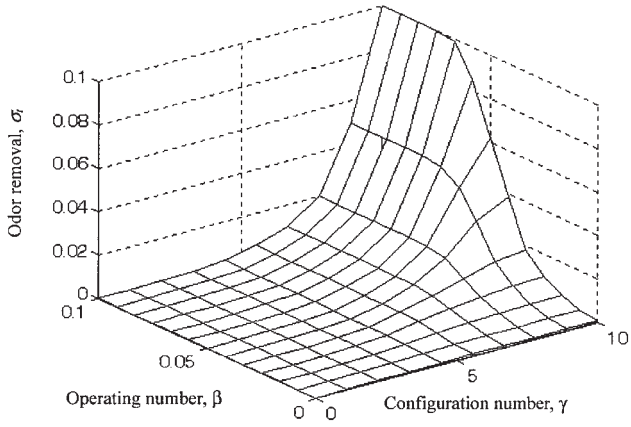

Figure 9. Odor gas removal against operating number ($\beta = V_L / H_A V_G$) and configuration number ($\gamma = K_t A_m / V_G$) for the pure physical stripping process.

The procedures to design the hollow fiber membrane module for the purification of indoor air may be described as follows:

(1) Calculation of the odor gas removal, σ_t by Eq. 24 from the air flow rate through an air conditioner, V_G, the concentration of odor gas that makes people uncomfortable, C_{Ag}, and the formation rate of odor gas from the furniture or human bodies, υ_f;

(2) Calculation of the operating number, β of the module under designed the environmental condition, $\beta = V_L / H_A V_G$;

(3) Determination of the configuration number of the module, γ from Figure 9;

(4) Determination of the membrane area needed for the indoor air purification by $A_m = V_G \gamma / K_t$. Associated with the packing density of hollow fibers, the volume of the hollow fiber membrane module can be obtained.

As an example, the hollow fiber membrane module for the removal of ammonia from indoor air has been computed. The parameter values for the calculation are listed in Table 4. As a result, the membrane area needed for the effective removal of ammonia is only $A_m = 0.0169$ m^2, or the volume of the module is about 8.44×10^{-6} m^3. Of course, the actual membrane area of the membrane module for indoor air purification should be more than this value because the solubility of other odor gases may be much less than that of ammonia.

Conclusions

A mathematical model for the odor gas removal using hollow fiber membrane modules has been developed, with which

Table 4. Parameter Values for the Design of Hollow Fiber Membrane Modules to Remove Ammonia from Indoor Air

Starting temperature	309 K
Target temperature	293 K
RH of the indoor air	90%
Henry constant of ammonia	$H_A = 7.03 \times 10^{-4}$
Overall mass transfer coefficient	$K_t = 1 \times 10^{-2}$ m/s
Volumetric flow rate of gas through air-conditioner	*$V_G = 0.167$ m^3/s
Formation rate of ammonia	1.67×10^{-10} m^3/s
Bearable ammonia concentration	1 ppm
Packing density of hollow fibers	2000 m^2/m^3

*The value was estimated for an office space for 20 people.[18]

the performances of the hollow fiber membrane modules have been analyzed under various operating conditions. In order to have the optimum removal of the odor gas from gas streams, it is necessary to increase not only the flow rate of stripping solution and the reactant concentration, but also to provide enough membrane areas. Compared with the pure physical absorption, the addition of chemical additive in stripping solution shows considerable increase in removal of the odor gas. The optimum values of the flow rate of stripping solution and the reactant concentration for odor removal using the hollow fiber membrane modules may be determined by Eq. 23. Using Na_2CO_3 aqueous solution as the stripping solution, a very high removal of H_2S from gas stream may be obtained. Higher operating pressures favor the removal of H_2S from gas streams. All the experimental data can be estimated satisfactorily with this mathematical model. The hollow fiber membrane modules can also be applied to the purification of indoor air by attaching to air conditioners, where the condensed water formed during the refrigeration acts as the stripping solution. The membrane area needed for odor removal depends on its solubility or Henry's constant in water.

Acknowledgments

The authors gratefully acknowledge the research funding provided by EPSRC in the U.K. (grant No. GR/R57171).

Notation

A_m = membrane area, m^2
C_A = concentration of odor gas in the bulk stripping solution, mol/m^3
C_B = concentration of absorbing reactant in the bulk solution, mol/m^3
C_{Ag} = odor concentration in the gas stream, mol/m^3
C_{Af} = odor concentration in the gas feed, mol/m^3
C_{Bf} = reactant concentration in liquid feed, mol/m^3
D_{Am} = diffusivity of odor gas in the membrane, m^2/s
D_{Ag} = diffusivity of odor gas in gas phase, m^2/s
D_{Al} = diffusivity of odor gas in the stripping solution, m^2/s
D_{Bl} = diffusivity of the absorbing reactant in stripping solution, m^2/s
D_s = ID of the hollow fiber membrane module, m
d_e = characteristic diameter of the module, m
Gz = graetz number (where $d = 2R_i$)
H_A = Henry's coefficient of odor gas, $C_{Ag} = H_A \cdot C_{Al}$
K_t = the overall mass-transfer coefficient of the module, m/s
k_{Am} = membrane's mass-transfer coefficient, m/s
L = effective length of the hollow fibers, m
L_p = effective pore length of the membrane skin, m
N_A = permeation molar flow rate of odor gas, mol/s
n = number of hollow fibers in the module
P = operating pressure, Pa
R_i = inner radius of the hollow fiber membrane, m
R_o = outer radius of the hollow fiber membrane, m
r_m = mean pore radius of the membrane, m
$\mathcal{R}$ = Ideal gas constant, $\mathcal{R} = 8.314$ J/mol K
Sh = Sherwood number, defined in Table 2
Sh_t = overall Sherwood number of the module,
u_m = average velocity of gas stream, m/s
V_G = volumetric flow rate of gas stream, m^3/s
V_L = volumetric flow rate of stripping solution, m^3/s
X = dimensionless concentration

Greek letters

β = operating number for the pure physical stripping process, $\beta = V_L / H_A V_G$
β_1 = feed modulus defined in Table 2
β_2 = concentration modulus defined in Table 2
γ = configuration number for the purely physical stripping process, $\gamma = K_r A_m / V_G$
γ_1, γ_2 = dimensionless number defined in Table 2
δ = thickness of the liquid boundary layer, m
δ_r = depth of reaction plane, m
ε_p = porosity of the membrane skin
η = dimensionless radius of the hollow fiber membrane
ξ = dimensionless fiber length
σ = standard deviation of membrane pores
σ_t = overall removal of odor gas
ϕ = packing fraction of hollow fiber in the module

Subscript

A = odor gas
B = absorbing reactant
f = feed stream
g = gas phase
l = liquid phase
m = membrane

Literature Cited

1. Strauss W. *Industrial Gas Cleaning*. 2nd ed. In: International series in chemical engineering, Oxford: Pergamon Press, 1975.
2. Zhang Q, Cussler EL. Microporous hollow fibers for gas absorption I: Mass transfer in the liquid. *J Membr Sci.* 1985;23:321-322.
3. Zhang Q, Cussler EL. Microporous hollow fibers for gas absorption II: Mass transfer across the membrane. *J Membr Sci.* 1985;23:333-345.
4. Yang M, Cussler EL. Designing hollow fiber contactors. *AIChE J.* 1986;32:1910-1916.
5. Cooney D, Jackson C. Gas absorption in a hollow fiber device. *Chem Eng Commun*. 1989;79:153-163.
6. Ahmed T, Semmens MJ. Use of sealed end hollow fibers for bubbeless membrane aeration: Experimental studies. *J Membr Sci*., 1992;69:1-10.
7. Kreulen H, Smolders CA, Versteeg GF, van Swaaij WPM, Determination of mass transfer rates in wetted and nonwetted microporous membranes. *Chem Eng Sci*. 1993;48:2093-2102.
8. Kreulen H, Smolders CA, Versteeg GF, van Swaaij WPM, Microporous hollow fiber membrane modules as gas-liquid contactors: Part 1. Physical mass transfer processes. *J Membr Sci*. 1993;78:197-216.
9. Costello MJ, Fane AG, Hogan PG, Schofield RW. The effect of shell side hydrodynamics on the performance of hollow fiber modules. *J Membr Sci*.1993;80:1-11.
10. Li K, Tai MSL, Teo WK, Design of a CO_2 scrubber for self-contained breathing systems using a microporous membrane. *J Membr Sci.* 1994;86:119-125.
11. Deshmukh SP, Li K. Effect of ethanol composition in water coagulation bath on morphology of PVDF hollow fiber membranes. *J Membr Sci.*, 1998;150:75-85.
12. Kong J, Li K. An improved gas permeation method for characterising and predicting the performance of microporous asymmetric hollow fiber membranes used in gas absorption. *J Membr Sci*. 2001;182:271-281.
13. Mochizuki S, Zydney AL. Theoretical analysis of pore size distribution effects on membrane transport. *J Membr Sci*. 1993;82:211-227.
14. Zydney AL, Aimar P, Meireles M, Pimley JM, Belfort G. Use of the log-normal probability density function to analyze membrane pore size distributions: Functional forms and discrepancies. *J Membr Sci.* 1994; 91:293-298.
15. Li K, Kong J, Tan XY. Design of hollow fiber membrane modules for soluble gas removal. *Chem Eng Sci*. 2000;55:5579-5588.
16. Astarita G, Savage DW, Bisio A. *Gas Treating with Chemical Solvent*, New York: John Wiley & Sons, Inc., 1983.
17. Li K, Tan XY. Development of membrane-UV reactor for dissolved oxygen removal from water. *Chem Eng Sci*. 2001;56:5073-5083.
18. ASHRAE standards, URL: http://www.ashrae.com/standards.

Manuscript received June 9, 2004, and revision received Aug. 11, 2004.